Vol. 398: 157–171, 2010
doi: 10.3354/meps08346

MARINE ECOLOGY PROGRESS SERIES
Mar Ecol Prog Ser

Published January 5

OPEN ACCESS

Ocean acidification alters skeletogenesis and gene expression in larval sea urchins

Michael J. O'Donnell[1,4], Anne E. Todgham[2,5], Mary A. Sewell[3], LaTisha M. Hammond[2], Katya Ruggiero[3], Nann A. Fangue[2,6], Mackenzie L. Zippay[2,7], Gretchen E. Hofmann[1,2,*]

[1]Marine Science Institute, University of California, Santa Barbara, California 93106, USA
[2]Department of Ecology, Evolution and Marine Biology, University of California, Santa Barbara, California 93106, USA
[3]School of Biological Sciences, University of Auckland, Private Bag 92019, Auckland, New Zealand

[4]*Present address:* Friday Harbor Laboratories, University of Washington, Friday Harbor, Washington 98250, USA
[5]*Present address:* Department of Biology, San Francisco State University, San Francisco, California 94132, USA
[6]*Present address:* Department of Wildlife, Fish & Conservation Biology, University of California, Davis, California 95616, USA
[7]*Present address:* Medical University of South Carolina, Hollings Marine Laboratory, Charleston, South Carolina 29412, USA

ABSTRACT: Ocean acidification, the reduction of ocean pH due to the absorption of anthropogenic atmospheric CO_2, is expected to influence marine ecosystems through effects on marine calcifying organisms. These effects are not well understood at the community and ecosystem levels, although the consequences are likely to involve range shifts and population declines. A current focus in ocean acidification research is to understand the resilience that organisms possess to withstand such changes, and to extend these investigations beyond calcification, addressing impacts on other vulnerable physiological processes. Using morphometric methods and gene expression profiling with a DNA microarray, we explore the effects of elevated CO_2 conditions on *Lytechinus pictus* echinoplutei, which form a calcium carbonate endoskeleton during pelagic development. Larvae were raised from fertilization to pluteus stage in seawater with elevated CO_2. Morphometric analysis showed significant effects of enhanced CO_2 on both size and shape of larvae; those grown in a high CO_2 environment were smaller and had a more triangular body than those raised in normal CO_2 conditions. Gene expression profiling showed that genes central to energy metabolism and biomineralization were down-regulated in the larvae in response to elevated CO_2, whereas only a few genes involved in ion regulation and acid-base balance pathways were up-regulated. Taken together, these results suggest that, although larvae are able to form an endoskeleton, development at elevated CO_2 levels has consequences for larval physiology as shown by changes in the larval transcriptome.

KEY WORDS: Biomineralization · Skeletogenesis · CO_2 · *Lytechinus pictus* · Microarray · Echinoplutei · Morphometrics · Transcriptomics

INTRODUCTION

Ocean acidification (OA), the reduction of ocean pH due to the absorption of anthropogenic CO_2 into surface seawaters (Caldeira & Wickett 2005), has been identified as perhaps the greatest anthropogenic threat to marine ecosystems (Halpern et al. 2008). Changes in the pH of the world's oceans are considered inevitable on the basis of levels of CO_2 already released into the atmosphere (Doney et al. 2009). Current predictions are that pH may decrease by 0.4 units by the year 2100 (Skirrow & Whitfield 1975, Caldeira & Wickett 2005, McNeil & Matear 2006, Doney et al. 2009), a situation that will have unquestioned negative biological consequences for those marine organisms which biomineralize calcium carbonate into hard parts such as shells and skeletons. Studies have highlighted effects on marine calcifiers from a range of marine

*Corresponding author. Email: hofmann@lifesci.ucsb.edu

ecosystems including deep-sea and tropical corals (e.g. Guinotte et al. 2006, Hoegh-Guldberg et al. 2007, Anthony et al. 2008, Cooper et al. 2008), coralline algae (e.g. Kuffner et al. 2007), a variety of benthic invertebrates (e.g. Kurihara & Shirayama 2004, Shirayama & Thornton 2005, Dupont et al. 2008, Hall-Spencer et al. 2008), and high-latitude planktonic invertebrates (e.g. Orr et al. 2005). These studies have clearly demonstrated the potential for deleterious effects of OA on a number of processes, including calcification, growth, reproduction, and development (reviewed in Fabry et al. 2008).

Significant gaps still exist in our knowledge of the physiological mechanisms underlying measured morphological changes, and how these species-level responses will be transmitted to the community and ecosystem levels (Doney et al. 2009). Although species-level variation in response to OA has been documented in rates of calcification (e.g. Fabry 2008), and predator-induced shell thickening (e.g. Bibby et al. 2007), the degree of plasticity within other vital cellular processes such as protein synthesis or stress tolerance is unknown. These observations underscore the need to focus on physiological plasticity with sufficient resolution to understand organismal function under levels of acidification expected in the near future. One promising avenue is to look for plastic responses in gene expression patterns. Profiling the transcriptome—the group of all mRNAs in a cell—of an organism is a method to gain insight into global patterns of physiological change to assess organismal plasticity (e.g. Cossins & Crawford 2005, Gracey 2007) as well as to gauge response to changing environmental conditions (e.g. Place et al. 2008), including the identification of genes involved in biomineralization (Quinn et al. 2006).

Recent work on the sea urchin *Strongylocentrotus purpuratus* has shown that a number of genes in important cellular processes undergo expression changes in response to acidification (Todgham & Hofmann 2009), illustrating how the larval transcriptome is altered during development under potentially stressful environmental conditions. Specifically, that study detected no major stress signatures, as might be expected with a response such as the heat shock response, a classic up-regulation of genes in the larval defensome, a broad suite of stress-responsive genes. Rather, analysis of the genes that did change during development in early prism stage larvae suggested a global metabolic depression in the response to CO_2-acidified seawater (Todgham & Hofmann 2009).

Regular sea urchins are ideal study organisms, combining both ecological importance (Pearse 2006) with deep genomic resources (Sea Urchin Genome Sequencing Consortium 2006). Regular urchins are prolific grazers, exerting structuring effects on their communities (e.g. Hughes et al. 1987, Watanabe & Harrold 1991). Their larvae have a long period of planktonic development, during which they synthesize an endoskeleton composed of high-magnesium calcite, one of the more soluble calcium carbonate forms. The study of sea urchin development has a long history (Strathmann 1987), with detailed information available on the formation and timing of skeletogenesis (Wilt 2002) and the genes involved in biomineralization (Livingston et al. 2006) and stress resistance (Goldstone et al. 2006). Previous studies have shown that, while echinoplutei can successfully calcify skeletal segments under OA conditions (e.g. Kurihara et al. 2004, Clark et al. 2009) a number of processes can be affected. These include fertilization (Havenhand et al. 2008), skeletal formation (Kurihara & Shirayama 2004, Dupont et al. 2008), and other physiological capacities such as the tolerance of temperature stress (O'Donnell et al. 2009), which has also been observed in amphipods (Hauton et al. 2009).

To begin addressing the physiological mechanisms underlying morphological changes in response to conditions of OA, we have explored changes during development in *Lytechinus pictus*, a species from Californian coastal waters. Our experiments combine detailed analysis of the morphology of the larval endoskeleton, a calcium carbonate structure that is vital for larval movement, dispersal, and feeding, with changes in gene expression in echinopluteus stage larvae grown under conditions of enhanced CO_2. This enables us to discuss gross morphological changes in the context of the underlying physiological state of the organisms as revealed by their transcriptome. We have analyzed a portion of the larval transcriptome to determine responsiveness of a variety of biochemical pathways and cellular processes that are critical to metabolic activity and to biomineralization during development. We use a boutique oligonucleotide DNA microarray that is designed to assess the expression of over 1000 genes involved in several cellular processes, including biomineralization, in larval sea urchins (Todgham & Hofmann 2009). The gene expression patterns are combined with detailed metrics of larval morphology to create a more holistic view of how larval physiology and skeleton formation change during development under high CO_2 conditions.

MATERIALS AND METHODS

Conditions for CO_2 incubations. *Lytechinus pictus* larvae were raised in seawater treated with 3 different concentrations of CO_2. Seawater was pumped from 20 m depth off the University of California Santa Bar-

bara (UCSB) campus and delivered through a flowing seawater system to our laboratory. We aerated water in culture chambers with air that had been pre-mixed to different CO_2 concentrations, 540 and 970 parts per million (ppm). These levels were chosen from 2 predicted future scenarios of atmospheric CO_2 levels (IPCC 2001), and the pre-mixed air was purchased from a commercial supplier (Praxair). As a control, we used compressed air (~380 ppm CO_2). We did not assess water samples for detailed carbonate chemistry, but monitored pH of each chamber, as well as the header tanks and the incoming seawater using a Radiometer Analytical PHM240 pH meter calibrated with NBS (National Bureau of Standards) buffers. In the absence of detailed data regarding the CO_2 concentrations in our cultures, we have defined them as Control, Intermediate, and High, referring to the expected CO_2 levels.

To test the efficacy of our aeration, we subsequently conducted a follow-up experiment using the same culture chambers and similar larval densities. We measured the pH of the culture chambers potentiometrically (using an Orion 720A meter and a ROSS Ultra combination electrode calibrated with NBS buffers). Following the procedures of Dickson et al. (2007), we took a 500 ml water sample daily from each experimental bucket, fixed with mercuric chloride and stored in a sealed glass bottle. These samples were sent to the Marine Physical Laboratory at Scripps Institution of Oceanography for measurements of total alkalinity (TA) and dissolved inorganic carbon (DIC). Although TA and DIC are not direct measures of the original experimental conditions, this follow-up provided insight into the performance of our aeration system.

We estimated the potential CO_2 levels in the original experiment by using temperature and salinity data gathered by the Southern California Coastal Ocean Observing System (SCCOOS) station at Stearns Wharf (Santa Barbara, CA, approximately 14 km from our seawater intake) during the dates of the experiment. We had no source for local TA data; instead, we estimated TA using the method of Lee et al. (2006, with coefficients for the North Pacific). The salinity during this period averaged 33.5 (SD of 0.01); the temperature averaged 17.7°C (SD 0.48°C). These values resulted in a calculated TA of 2291 µmol kg^{-1} seawater. These data were then used to calculate the difference in dissolved CO_2 between treatments using the program CO2SYS (Pierrot et al. 2006) (constants from Mehrbach et al. 1973; NBS buffers). We used the chemistry results from our follow-up experiment to explore the validity of our assumed salinity and TA and found that theoretical TA was within 3% of the measured value.

Maintenance of larval cultures. Adult *Lytechinus pictus* were collected in July 2007 on SCUBA from a depth of ~10 m near Los Angeles, CA, by a biological supply company (Marinus Scientific). Exact collection temperature was not known, but sea surface temperatures (SSTs) near the area of collection averaged ~20°C during the weeks prior to collection (SCCOOS data, Santa Monica, CA). Urchins were maintained in flowing seawater at UCSB at ambient temperature (from ~15 to ~18°C) and fed kelp until use. Spawning was induced by coelomic injection of 0.5 M KCl, and eggs were collected in 0.35 µm-filtered seawater. The eggs from 5 females were combined in approximately equal concentrations, filtered through 125 µm mesh and gently stirred to mix in 1 l of water. Sperm from a single male was collected in the same way; 40 µl was diluted into 60 ml of filtered seawater and from 5 to 10 ml was added to the egg mixture; thus, all the larvae are half-siblings. Samples were examined for the presence of fertilization membranes, and >95% of the eggs were fertilized within 5 minutes. Immediately following fertilization, embryos were filtered through a 64 µm mesh filter, rinsed with filtered seawater to prevent polyspermy, and split into 12 culture chambers providing 4 replicates of the 3 CO_2 treatments. Initial culture densities were approximately 20 individuals ml^{-1}; through repeated sample collections these densities dropped (~19 ml^{-1} at 53 h, 13 ml^{-1} at 70 h, 8 ml^{-1} at 142 h). The culture chambers were designed to allow aeration bubbles to mix with the culture water without vigorous turbulence that could damage the larvae. Each chamber was constructed from two 20 l buckets, one nested inside the other. The inner bucket had 12 holes (55 mm in diameter) covered with panels of 64 µm mesh to allow free water exchange between the buckets while keeping the larvae contained. The outer bucket had a standpipe running from the sump below the inner bucket, which returned water, through a perforated pipe, to the inner bucket. Gas bubbled through the standpipe at a rate of ~70 ml min^{-1}, providing a lifting force in the pipe, which simultaneously aerated the water with the selected gas mixture and gently stirred the culture vessel. Drippers provided a constant flow of fresh 0.35 µm-filtered seawater to the buckets at a rate of 0.5 l h^{-1}. The drippers were fed from header tanks (approximately 5 l) which were also aerated with the treatment gas. Chambers were held in a water bath maintained at 18.5°C.

At 48, 53, 70, and 142 h after fertilization, ~200 larvae were sampled from each of the 12 culture chambers. Culture densities were quantified by stirring cultures and counting the larvae in a sample of between 100 and 250 µl, then scaling up to the total volume. From this density calculation, we determined the appropriate volume of water which we removed by dipping a beaker and gently pouring through a 64 µm mesh screen, returning the water to the bucket. The

larvae remaining on the screen were removed by pipette and preserved with 1% formalin solution. During this time the larvae advanced from late prism to well-developed 4-arm echinoplutei. At the 48 h time point, a sample of ~40 000 larvae was removed from each culture in the Control and High treatments and stored in 1 ml TRIzol® Reagent (Invitrogen) at −80°C for later RNA analysis (to maintain culture density, a similar sample was extracted from the Intermediate treatment, though it was not analyzed).

Morphometric methods. Larvae were photographed with a digital camera fitted to an Olympus BX-50 microscope (within 20 d of fixation to avoid dissolution of the skeleton as a result of long-term contact with formalin). Fixed larvae were pipetted onto a flat microscope slide, and a cover slip, with modelling-clay feet on the corners, was placed over them. The first 30 larvae found on the slides in the correct orientation, ventral side down, were photographed. Images were analyzed using ImageJ (NIH), and 9 measures were taken (shown in Fig. 1A): body length from the tip of the body to the ventral arch (BLV), length of left and right body rod (LBR, RBR), post-oral arms (LPO, RPO), and transverse rods (LTR, RTR) measured on both the left and right sides; the body width was measured at the midline of the body, through the center of the gut (BW) and at the tips of the body rods (BWT). As a proxy for total skeletal growth we summed the lengths of the body rods, post-oral arms, and transverse rods on the left and right sides ('total larval skeleton', TLS). While this is not actually a measure of all the skeletal segments in the larvae, since it does not include those out of the plane of the photograph, it provides a measure of growth of multiple areas of the body.

Statistical analysis of morphometrics. Morphometric analyses of echinoplutei were conducted at each time point (48, 53, 70, and 142 h post-fertilization) and at all time points simultaneously. To examine variation in larval shape with CO_2 treatment, we performed non-metric multi-dimensional scaling (nMDS) using a Euclidean distance matrix on 5 un-transformed morphometric parameters (LTR + RTR, BLV, RPO, RBR, and BWT) using PRIMER v 6.1.1.11 (Plymouth Marine Laboratory). For each time point a permutational multivariate analysis of variance (PERMANOVA) was conducted using the PERMANOVA+ add-on (v 1.01) in PRIMER with CO_2 treatment as a fixed factor and culture chamber nested within CO_2 treatment as the random factor. The PERMANOVA analysis used 9999 permutations under a reduced model, and a companion test was run using the PERMDISP routine to test for the homogeneity of multivariate dispersions between CO_2 treatments using deviations from centroids and 9999 permutations (Anderson et al. 2008). When differences were detected in larval morphometrics between CO_2 treatments by PERMANOVA, additional pairwise tests were conducted using the square root of the pseudo-*F* statistic (*t*-test) with 9999 permutations as in the main test. Finally, the similarity percentage analysis (SIMPER) routine in PRIMER was used to identify the relative contributions of each morphometric parameter to the differences between CO_2 treatments.

Univariate analyses were conducted using a mixed-model ANOVA with REML estimation using JMP v7. As in the multivariate analyses, CO_2 treatment was a fixed effect, and culture chamber was a random effect nested within treatment. Where significant effects of CO_2 treatment were detected, Tukey-Kramer HSD pairwise comparisons ($\alpha = 0.05$) were used to elucidate the degree to which individual treatment groups were different from each other. Data were normally distributed and were not transformed for analysis.

Gene expression profiling with oligonucleotide microarrays. ***Strongylocentrotus purpuratus microarray construction:*** Microarray analysis was performed using a custom-designed oligonucleotide microarray developed to screen the expression patterns of genes central to the calcification process, the cellular defensome, development, energy metabolism, translational control, and cell signaling in purple sea urchins (Sea Urchin Genome Sequencing Consortium 2006). The construction of the *S. purpuratus* microarray used in this experiment is reported by Todgham & Hofmann (2009). While this array was designed using sequence from the purple urchin *S. purpuratus*, we were very successful in cross hybridizing with *Lytechinus pictus*. There was >80% probe hybridization with *L. pictus* cDNA and a high degree of differential expression.

RNA extraction and microarray hybridization: Total RNA was extracted from a pooled sample of approximately 40 000 early 4-arm urchin larvae (48 h post-fertilization) from each of the 4 replicate cultures of the Control and High CO_2 culture treatments (8 samples in total). Total RNA was isolated using the guanidine isothiocyanate method (Chomczynski & Sacchi 1987) using TRIzol®. Following extraction, RNA was processed through an additional clean-up step to remove tRNA and small-sized RNA degradation products using glass-fiber filter columns following the manufacturer's instructions (Applied Biosystems, and Ambion). RNA was quantified spectrophotometrically using an ND-1000 UV/ visible spectrophotometer (NanoDrop Technologies) and electrophoresed on a 1.5% w/v agarose gel to verify RNA integrity. RNA was stored at −80°C.

First strand cDNA was synthesized from 10 µg of total RNA using anchored oligo($dT_{23}V$) and pdN6 random hexamer primers, amino-allyl dUTP, and SuperScript III reverse transcriptase (Invitrogen). Each sample was labeled by indirect coupling with either Alexafluor 555 or Alexafluor 647 succinimidyl ester

dyes (Invitrogen). The cDNA samples were checked spectrophotometrically (Nanodrop Technologies) to ensure high quality cDNA synthesis (>600 ng) and dye incorporation (>8.0 pmol dye μg^{-1} cDNA) before continuing to slide hybridization. The larval cDNA samples from each treatment were competitively hybridized on each microarray following a balanced incomplete block design with respect to the assignment of treatments to arrays. In this way, differential expression between all pairs of treatments is estimated with equal precision. Although dye swaps of technical replicates were not used, treatment and dye effects are orthogonal to one another, i.e. treatment effects can be estimated independently of dye effects.

Normalization and statistical analysis of microarray data: Data from the 6 microarrays were extracted using GenePix Pro 4.0 software (Molecular Devices). The data discussed in the present manuscript have been deposited in the National Center for Biotechnology Information (NCBI) Gene Expression Omnibus (GEO; www.ncbi.nlm.nih.gov/geo/) and are accessible through the GEO Series Accession Number GSE13655. Normalization and data analysis were completed using R (R Development Core Team 2008) with the limma software package (Smyth 2005). Intensity-dependent lowess normalization is the most commonly used method for eliminating labeling bias in dual channel microarray platforms (Yang et al. 2002). The targeted array used in this experiment is designed to be a 'stressor'-responsive chip with 50% of the genes attributed to the defensome, biomineralization pathways, acid-base balance, and apoptosis. To avoid violating assumptions of the number or degree of symmetry of differentially expressed genes, a global normalization for dye-bias was applied on a probe-by-probe basis, after averaging over log-ratios from replicate probes within arrays, by including a dye effect in the linear model. Analysis of differential expression was based on empirical Bayes moderated *t*-statistics (Smyth 2004). A table was generated of the mean log fold change (FC) of gene expression and the corresponding moderated standard error (SE) of the top 100 probes that demonstrated the greatest expression differences between the Control and High CO_2 treatments (Table 3). These moderated SEs were then used to back transform the log FCs to the upper and lower limits of fold changes in expression.

RESULTS

Culture conditions

During the ~150 h culture period, the pH of the seawater in the Control, Intermediate, and High CO_2 treatments was 7.93 ± 0.01, 7.87 ± 0.02, and 7.78 ± 0.03, respectively (mean ±1 SE). Thus, the High and Intermediate CO_2 treatments were correspondingly an average of 0.15 pH and 0.06 units lower than the Control. Because we did not take samples for complete chemical analysis, we could not directly ascertain whether the culture chambers were in equilibrium with the aeration gas. However, follow-up analysis of our replicated culture conditions demonstrated that our potentiometric pH readings accurately described the differences between our treatment conditions. Calculations with CO2SYS showed that our dissolved CO_2 levels were considerably higher than anticipated and not in equilibrium with the aeration gas. The incoming seawater supplying the experiment generally had a pH that was between the Control and Intermediate treatments, suggesting that this water had high levels of dissolved CO_2, likely as a result of biological activity within the supply pipes. Thus, our Control treatment is not a true representation of ambient ocean conditions. Nevertheless, the reduction in pH between our Control and High treatments indicates that we were effective in altering the CO_2 levels within the water and that the pH measures are well within the range predicted for future oceans.

Larval morphometrics

Lytechinus pictus larvae raised in Intermediate and High CO_2 conditions were smaller than (Fig. 2A,B) and were separated in multivariate space from the controls at all 4 time points examined (Figs. 3 & 4). Permutational MANOVA showed that there were significant differences in larval morphology between CO_2 treatments at 48, 53, and 70 h after fertilization; however, at 142 h, the p-value was marginally non-significant (p = 0.052, Table 1). At 48 h, 2 morphometric parameters reflecting size (RPO, RBR) explained from 50 to 60% of the squared Euclidean distance between CO_2 treatments (Table 2). However, after this time the shape variables (LTR + RTR and BWT) combined with the size measurement (RPO) explained over 80% of the differences (Table 2). Echinoplutei raised in elevated CO_2 conditions generally had shorter larval arms and a thinner, more triangular shaped larval body (Fig. 1).

During the course of the experiment *Lytechinus pictus* larvae in all CO_2 treatments showed growth, even in the absence of food, with increased length in the post-oral arm (RPO, Fig. 2A) and a shift towards the left in the location of the data cloud in 2-dimensional nMDS plots on the same scale (Fig. 4). However, the multivariate analysis also reveals significant variation in larval morphometrics at the 2 levels below the main effect (CO_2 treatment). For the

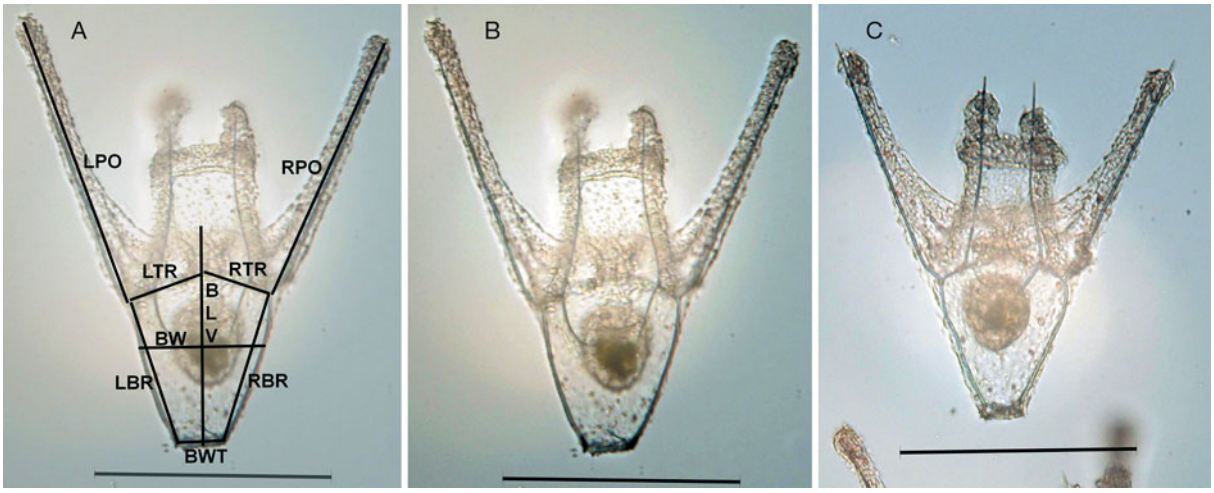

Fig. 1. *Lytechinus pictus.* (A) Morphometric parameters measured on 142 h larvae. BLV = length from tip to ventral arch; LBR, RBR = length of left and right body rod; LPO, RPO = length of left and right post-oral arm; LTR, RTR = length of left and right transverse arms; BW = length of body width at midline, BWT = length of body width at tip. Total skeleton (TLS) was calculated by summing (LBR + RBR + LPO + RPO + LTR + RTR). (B,C) Representative larvae from the Control (B) and High (C) CO_2 treatments. Photographs were chosen with RPO and RBR approximately median for their treatment group. Scale bars = 250 µm

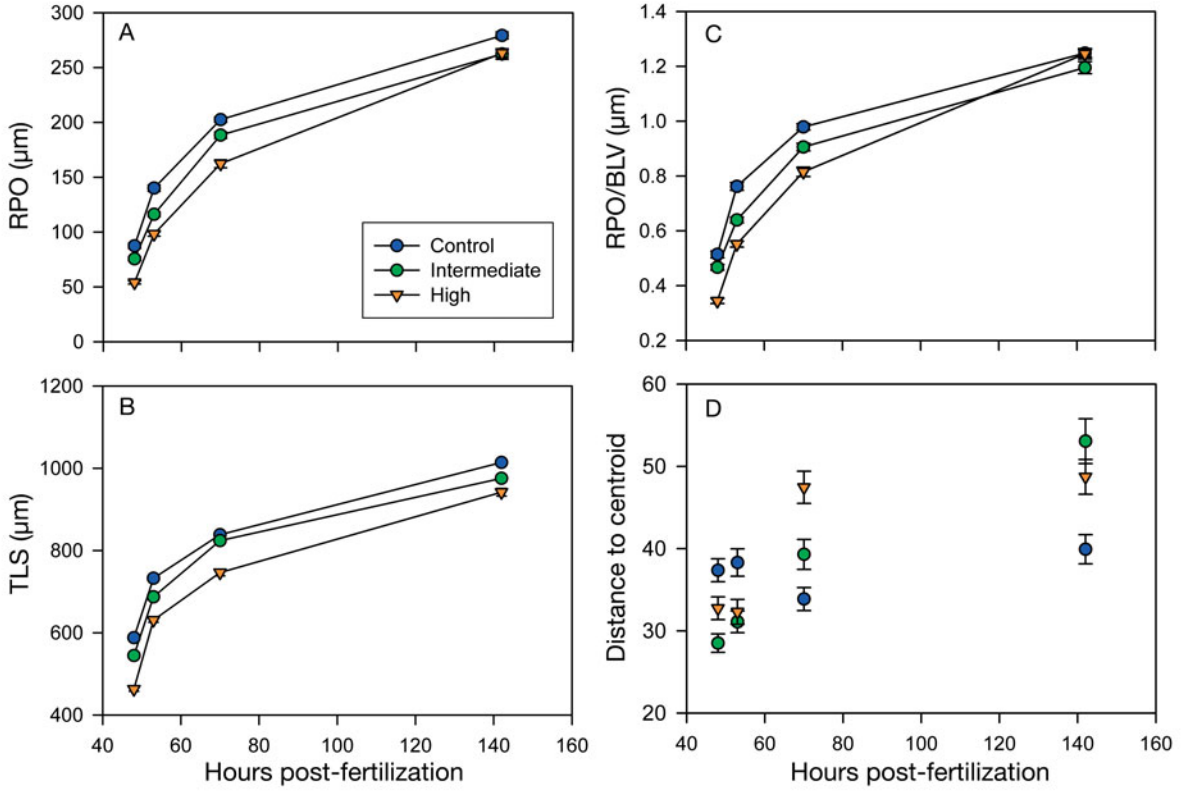

Fig. 2. *Lytechinus pictus.* Growth of larvae under different CO_2 conditions. (A) RPO length (µm). (B) TLS length (µm). (C) Proportional arm length (µm) relative to body size (RPO normalized by BLV). Data are means (±SE) of all replicate larvae from each treatment with individual culture chambers combined. (D) Distance to the centroid in 2-dimensional non-metric multidimensional scaling (nMDS) analysis. See Fig. 1 for definitions

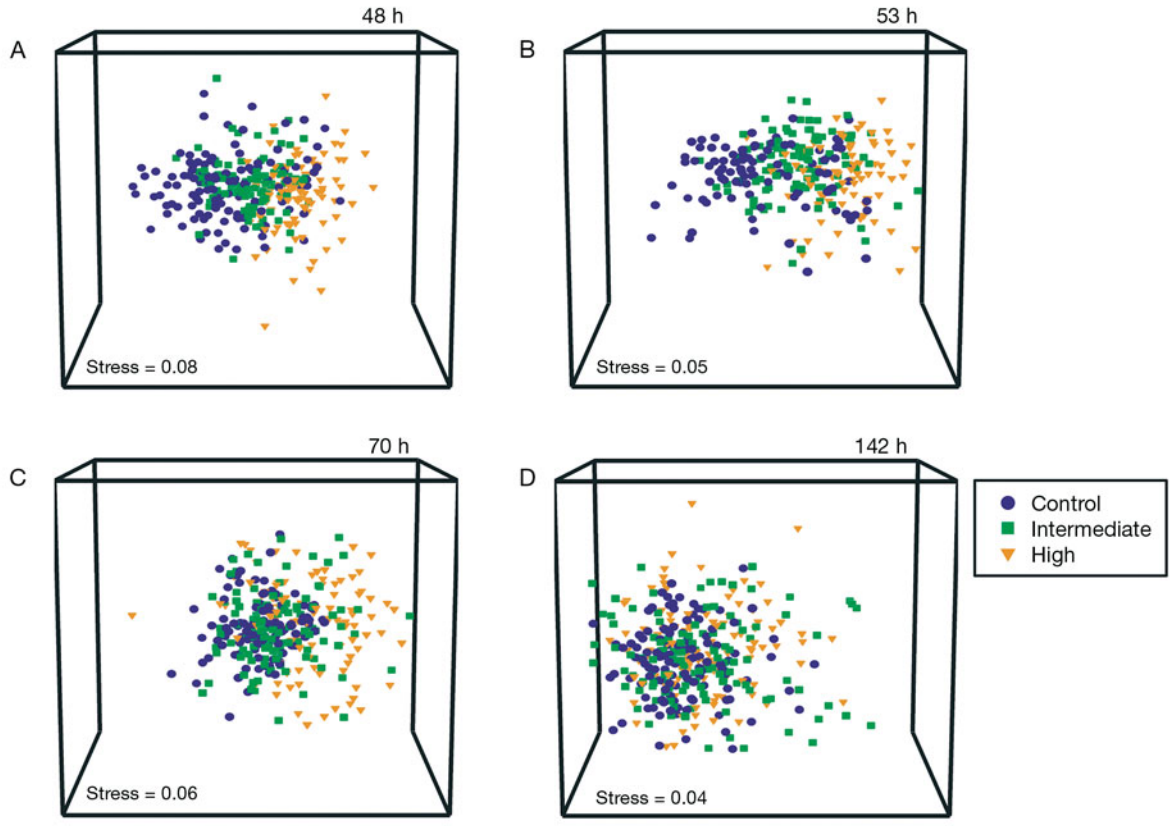

Fig. 3. *Lytechinus pictus.* Effect of enhanced CO_2 on echinoplutei morphometrics: multi-dimensional scaling (MDS) plots of the larvae from (A) 48 h, (B) 53 h, (C) 70 h, and (D) 142 h time points, analyzed separately. Analysis conducted on 5 larval metrics (BLV, RBR, RPO, LTR + RTR, BWT; see Fig. 1 for definitions)

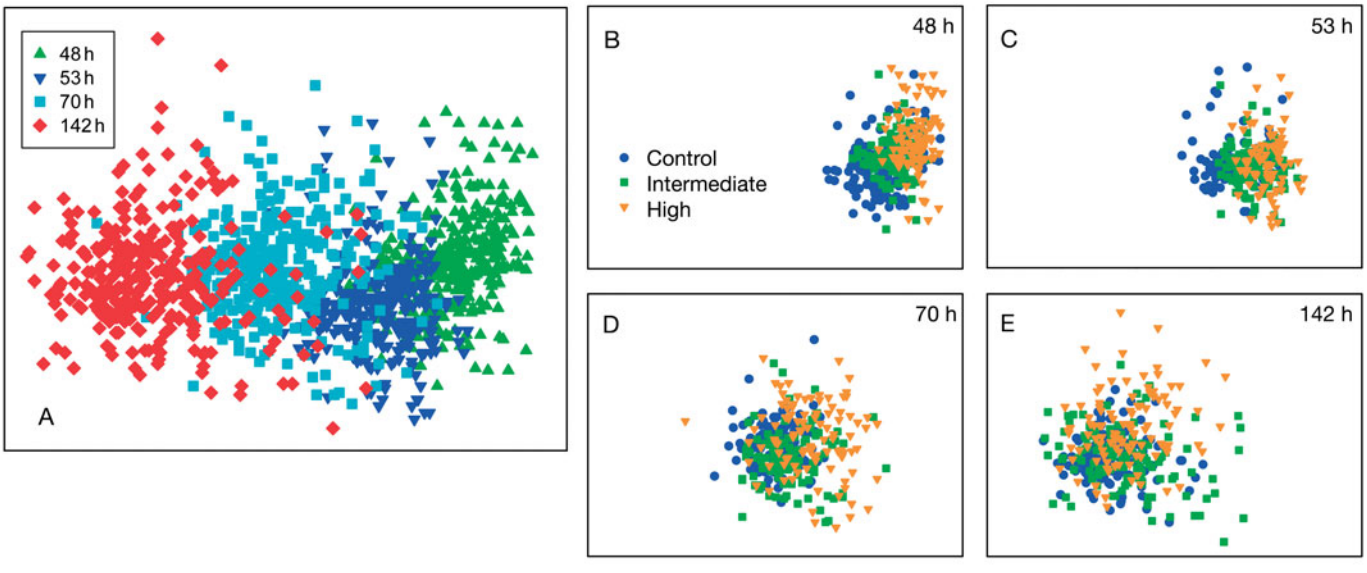

Fig. 4, *Lytechinus pictus.* Effect of enhanced CO_2 on echinoplutei morphometrics: MDS analysis of the 4 time points (48, 53, 70, 142 h) simultaneously. (A) Multi-dimensional scaling (MDS) plot color-coded by time point. (B–E) MDS plots showing the 48, 53, 70, and 142 h points seperately, color-coded by CO_2 treatment concentration. All MDS plots are plotted on the same linear scale. Two patterns are apparent: (1) larvae in the enhanced CO_2 treatments, although growing, are always smaller and maintain their position relative to the control treatment in multivariate space through time; (2) with the increase of exposure time to CO_2, there is more variation between larvae in both treatments, suggesting some degree of individual response to acidification

Table 1. *Lytechinus pictus.* Permutational multivariate analysis of variance based on Euclidean distance for echinoplutei cultured in different CO_2 treatments (C = Control, I = Intermediate, H = High) and with Culture nested within CO_2 treatment (Culture[CO_2 treatment]). PERMANOVA and pair-wise tests were run with 9999 permutations under a reduced model. Estimates of components of variation are given as the square root of the Euclidean distance and provide a measure of the relative importance of the terms in the overall model (Anderson et al. 2008). Significant results are shown in bold. Underlining in pairwise comparisons shows CO_2 treatments that are not significantly different

Time (h)	CO_2 treatment			Culture (CO_2 treatment)			Pairwise comparisons for CO_2 treatment				Estimated components of variation		
	F	df	p	*F*	df	p	Compare	*t*	p		CO_2	Culture	Residual
48	4.246	2,9	**0.035**	14.339	9,316	<0.001	C vs. I	0.949	0.368	C I H	20.179	21.596	30.865
							C vs. H	2.536	**0.043**				
							I vs. H	2.476	**0.013**				
53	4.062	2,9	**0.048**	7.985	9,274	<0.001	C vs. I	1.366	0.194	C I H	17.274	18.391	33.661
							C vs. H	2.478	0.058				
							I vs. H	2.602	**0.033**				
70	4.691	2,9	**0.029**	6.975	9,317	<0.001	C vs. I	1.454	0.154	C I H	19.944	19.206	41.087
							C vs. H	2.751	**0.038**				
							I vs. H	1.924	0.106				
142	2.402	2,9	0.052	5.528	9,342	<0.001	C vs. I	1.042	0.346	C I H	13.044	19.925	50.793
							C vs. H	2.754	**0.003**				
							I vs. H	1.279	0.205				

nested factor Culture(CO_2 treatment), while there are significant differences in larval morphology between cultures at all times, the value of the estimated variance component remains approximately constant (Table 1). In contrast, as the time to which larvae are exposed to enhanced CO_2 increases, there is a greater degree of variation at the level of individual larvae. This is shown by both the increased value for the residual variance component over time (Table 1) and by the increased deviation from centroid in the Intermediate and High CO_2 treatments at 70 and 142 h (Fig. 2D).

Univariate analyses on the 5 morphometric parameters used in the multivariate analysis were used to identify changes in specific skeletal rods under elevated CO_2 conditions (Table 3). Additionally, we calculated the ratio of RPO:BLV which measures the length of feeding structure relative to larval size, and total larval skeleton (TLS) which is an index of the amount of biomineralization in each larva. *Lytechinus pictus* larvae cultured in High CO_2 conditions produced a significantly smaller larval skeleton than in control conditions (e.g. TLS at 70 h was 10% smaller in High vs. Control larvae, Fig. 2B, Table 3), driven in part by significantly smaller lengths of RPO (almost 20% smaller at the 70 h time point) and body width (LTR + RTR) in the enhanced CO_2 treatments at most time points (Fig. 2A, Table 1). Larvae in the High CO_2 treatment furthermore have reduced capabilities to capture food, with significantly shorter arms for a given body size at the 48, 53, and 70 h time points (Table 3, Fig. 2C).

Gene expression

Analysis of the microarray data revealed numerous genes in developing larvae that were transcriptionally responsive to High CO_2. Of the 100 features that showed the greatest fold changes in expression in a comparison of control versus CO_2-raised larvae, 79% were down-regulated and 21% were induced in the larvae raised in High CO_2. Genes were subsequently assigned to broad biological processes in order to determine the larger cellular pathways that were responsive to decreases in seawater pH that characterize OA. The 5 process groups that displayed the highest fold changes are shown in Table 4. For genes related to biomineralization and skeletogenesis, 8 genes were found to decrease in expression in response to High CO_2. These included genes that are part of the organic matrix of the endoskeleton, in this case, 2 spicule matrix proteins (*SM30-like* and *SM29*). In addition, genes involved in spicule formation (e.g. collagen *COLP3α* and *Cyclophilin*) and the binding of Ca^{2+} (*Osteonectin*) were also down-regulated. For genes involved in metabolism and oxidative phosphorylation (e.g. *Atp5b*, *Cox4i1*, and *Slc25a4*), the expression patterns showed a near-unanimous 2-fold down-regulation in genes central to the electron transport chain. Combined with down-regulation in genes in the tricarboxylic acid (TCA) cycle (e.g. succinyl-CoA synthetase, *Suclg1;* and malate dehydrogenase, *Mdh1*), this pattern suggests a significant depression of metabolic activity, especially mitochondrial function, in larvae raised at High CO_2 conditions. Similar patterns of down-regula-

Table 2. *Lytechinus pictus.* Identification of the morphometric parameters, ordered in decreasing contribution, discriminating the CO_2 treatments at 48, 53, 70, and 142 h post-fertilization. Analysis was performed using the SIMPER routine in PRIMER v.6.1.11 on untransformed Euclidean distances, and a cut-off set at the point where the cumulative dissimilarity reached 90%. See Fig. 1 for abbreviations of morphometric parameters. $\bar{X}$ = mean length of the morphometric parameter in this CO_2 treatment (µm) and subscript values refer to the CO_2 treatment (C = Control, I = Intermediate, H = High). Contribution (%) and Cumulative (%) describe the contribution of each variable to the squared Euclidean distance

Treatment & morphometric parameter	$\bar{X}_C$	$\bar{X}_I$	$\bar{X}_H$	Contribution (%)	Cumulative (%)
48 h					
Control and Intermediate treatments (average squared distance = 2822.58)					
RPO	87.4	75.9	–	40.71	40.71
RBR	132	126	–	19.37	60.08
BWT	69.2	67.9	–	16.61	76.69
BLV	169	162	–	12.73	89.42
LTR + RTR	148	143	–	10.58	100.00
Control and High treatments (average squared distance = 4980.68)					
RPO	87.4	–	54	40.17	40.17
RBR	132	–	110	22.43	62.60
BLV	169	–	159	13.03	75.63
LTR + RTR	148	–	130	12.98	88.60
BWT	69.2	–	61.8	11.40	100.00
Intermediate and High treatments (average squared distance = 3159.19)					
RPO	–	75.9	54	31.65	31.65
RBR	–	126	110	22.50	54.15
BWT	–	67.9	61.8	16.26	70.41
LTR + RTR	–	143	130	14.82	85.23
BLV	–	162	159	14.77	100.00
53 h					
Control and Intermediate treatments (average squared distance = 3466.24)					
RPO	140	117	–	51.86	51.86
BWT	56.6	61.1	–	27.91	79.77
LTR + RTR	155	155	–	9.29	89.06
BLV	183	182	–	5.92	94.98
Control and High treatments (average squared distance = 4953.27)					
RPO	140	–	98.2	58.57	58.57
BWT	56.6	–	44	23.05	81.62
LTR + RTR	155	–	148	8.47	90.09
Intermediate and High treatments (average squared distance = 3082.90)					
BWT	–	61.1	44	38.32	38.32
RPO	–	117	98.2	34.41	72.73
LTR + RTR	–	155	148	12.35	85.08
RBR	–	150	146	7.73	92.81
70 h					
Control and Intermediate treatments (average squared distance = 3554.36)					
RPO	203	188	–	57.94	57.94
LTR + RTR	133	140	–	17.17	75.11
BWT	44.9	47.5	–	12.48	87.60
RBR	151	154	–	6.31	93.91
Control and High treatments (average squared distance = 5735.11)					
RPO	203	–	163	67.31	67.31
LTR + RTR	133	–	130	11.76	79.06
BWT	44.9	–	39	9.70	88.76
BLV	207	–	199	7.00	95.77
Intermediate and High treatments (average squared distance = 5503.34)					
RPO	–	188	163	59.78	59.78
LTR + RTR	–	140	130	15.06	74.84
BWT	–	47.5	39	12.02	86.86
BLV	–	208	199	7.68	94.53
142 h					
Control and Intermediate treatments (average squared distance = 5982.56)					
RPO	279	262	–	71.10	71.10
BWT	43.8	43.2	–	11.56	82.66
LTR + RTR	149	147	–	7.30	89.97
BLV	224	220	–	11.43	95.86
Control and High treatments (average squared distance = 5726.66)					
RPO	279	–	263	54.79	54.79
LTR + RTR	149	–	135	13.89	68.68
BWT	43.8	–	30.2	13.60	82.28
BLV	224	–	212	10.01	92.29
Intermediate and High treatments (average squared distance = 7069.33)					
RPO	–	262	263	62.45	62.45
BWT	–	43.2	30.2	12.20	74.65
LTR + RTR	–	147	135	10.89	85.54
BLV	–	220	212	7.80	93.35

tion were observed for 11 genes involved in the cellular defensome and 3 genes involved in the translation of newly synthesized proteins. Finally, genes involved in acid-base and ion regulation showed a mixed pattern of expression changes where some transporters were down-regulated (e.g. Na^+/K^+ ATPase), but other genes, such as *Atp2a1* (Ca^{2+} ATPase), *Atp13a3* (H^+/K^+ ATPase), and *Slc4a3* (bicarbonate transporter), were induced in larvae raised under High CO_2.

DISCUSSION

Over the next 100 yr, the best predictions are that atmospheric CO_2 levels will rise to 550–1000 ppm, an increase of at least 170 ppm over current conditions (IPCC 2001). Most scenarios predict a reduction in pH greater than that imposed by our High CO_2 treatment. In common with previous studies (e.g. Kurihara & Shirayama 2004, Dupont et al. 2008, Kurihara 2008, Clark

Table 3. *Lytechinus pictus.* Results of nested mixed model ANOVA for morphological parameters in echinoplutei between CO_2 treatments and for Culture(CO_2). See Fig. 1 for abbreviations of morphometric variables. RPO:BLV is RPO:BLV ratio. Separate analyses were conducted at the 4 time points. Pairwise comparisons were conducted when there was a significant effect of CO_2 treatment (C = Control, I = Intermediate, H = High) using Tukey-Kramer HSD ($p < 0.05$). Underlining in pairwise comparisons shows CO_2 treatments that are not significantly different. *Significant random effect of Culture(CO_2) as determined by the 95% confidence interval of the variance component including zero; NS indicates no significant differences found

Morphometric parameter	CO_2 treatment pairwise comparison	F_{CO_2}	p	Culture(CO_2) significance
BLV				
48 h	NS	0.795	0.481	*
53 h	NS	1.189	0.347	NS
70 h	C I H	4.437	**0.046**	NS
142 h	C I H	4.421	**0.048**	NS
TLS				
48 h	C I H	6.4593	**0.0182**	*
53 h	C I H	4.4321	**0.0455**	*
70 h	C I H	6.3975	**0.0187**	NS
142 h	C I H	5.0244	**0.0336**	NS
RPO				
48 h	C I H	5.187	**0.032**	*
53 h	C I H	5.046	**0.034**	*
70 h	C I H	5.071	**0.034**	NS
142 h	NS	1.048	0.389	NS
RBR				
48 h	C I H	5.473	**0.028**	*
53 h	NS	1.205	0.344	NS
70 h	NS	3.651	0.069	NS
142 h	C I H	12.241	**0.003**	NS
BWT				
48 h	NS	1.252	0.332	NS
53 h	NS	4.035	0.056	NS
70 h	NS	3.207	0.090	NS
142 h	NS	3.299	0.085	NS
LTR+RTR				
48 h	C I H	16.274	**0.001**	NS
53 h	C I H	5.464	**0.034**	NS
70 h	C I H	7.377	**0.012**	NS
142 h	C I H	10.166	**0.005**	NS
RPO:BLV				
48 h	C I H	5.254	**0.031**	*
53 h	C I H	5.709	**0.025**	*
70 h	C I H	4.578	**0.043**	NS
142 h	NS	0.396	0.684	NS

et al. 2009), our data suggest that there are indeed deleterious impacts of OA on the development of the larval endoskeleton, with smaller echinoplutei of altered shape produced in water with slightly reduced pH levels. In concert, the microarray data showed a number of significant changes in the larval transcriptome in response to High CO_2 — a down-regulation in the expression of genes that encode proteins central to skeletogenesis and energy metabolism, as well as an up-regulation of genes involved in acid-base regulation. Taken together, these changes indicate that enhanced CO_2 will alter larval development in significant and potentially ecologically important ways, adding additional stresses to what is already a vulnerable life history stage.

During their time in the plankton, larvae need to acquire sufficient food, avoid predators, and return to a suitable settlement habitat at the appropriate time. Any of these components of successful development risk disruption due to changes in morphology documented here. Swimming ability and stability in response to turbulence are dependent on body size and shape (Pennington & Strathmann 1990, Strathmann & Grünbaum 2006) and could affect success of individuals in the plankton. Echinoplutei rely on a ciliated band covering their arms for food capture and swimming ability (Strathmann 1971); reductions in arm size thus lead to reduced apparatus for feeding (Sewell et al. 2004). Hart & Strathmann (1994) observed that an 8% difference in the length of the ciliated band resulted in a 20% change in the rate at which water was cleared of food. The almost 20% reduction in RPO we documented at the 70 h time would result in larvae with diminished ability to capture food and locomote because they grew under elevated CO_2 conditions.

At least 2, non-exclusive, models could explain our morphometric results; either the larvae could be growing at a slower rate due to general effects of low pH on the progress of development, or the size and nature of skeleton could be stunted by direct deleterious effects of decreased pH on skeletogenesis. Either scenario would have implications for the ecology of these urchins. Smaller larvae may be preferentially preyed upon (e.g. Allen 2008) while a longer planktonic stage increases the length of time larvae are subjected to planktonic predators. Additionally, an increase in the length of time larvae must develop before they are competent to settle could disrupt connectivity between populations (e.g. Siegel et al. 2008). If changing larval size leads to smaller juveniles at settlement, such individuals would be at greater risk of predation during their early juvenile stage (Tegner & Dayton 1981). Our morphometric results are not able to differentiate between these 2 scenarios, however. The gene expression data, pointing to reductions in both metabolism

and biomineralization, suggest that both are probably happening.

Much of the work on skeletal growth of invertebrates under OA conditions has focused on external metrics such as linear growth (e.g. Kurihara & Shirayama 2004, Dupont et al. 2008) or total calcification (e.g. Langdon & Atkinson 2005). There have been a few gene expression studies (e.g. Hauton et al. 2009, O'Donnell et al.

Table 4. *Lytechinus pictus.* Fold changes in gene expression in early echinoplutei (48 h post-fertilization) that developed at High CO_2 compared with those in larvae raised at Control CO_2 levels. Data are presented as the upper (FCUL) and lower (FCLL) limits of fold change. Significant results are shown in **bold**

Gene name	Gene ID	Fold change (FCUL–FCLL)	p	Protein information
Metabolism — oxidative Phosphorylation				
Tricarboxylic acid cycle				
Suclg1	SPU_025397	−1.79 → −1.25	**0.0247**	Succinyl-CoA synthetase
Cs	SPU_024102	−1.62 → −1.13	0.0944	Citrase synthase
Mdh1	SPU_012677	−1.63 → −1.14	0.0862	Malate dehydrogenase
Pdha	SPU_011965	−1.54 → −1.08	0.1543	Pyruvate dehydrogenase
Electron transport chain				
Atp5b	SPU_005296	−1.78 → −1.24	**0.0256**	ATP synthase, F1 complex, beta subunit
Atp5j	SPU_001183	−1.70 → −1.19	0.0513	ATP synthase, F0 complex, subunit F6
Atp5g1	SPU_013052	−1.61 → −1.13	0.0946	ATP synthase, F0 complex, subunit C1
Atp5l	SPU_013135	−1.51 → −1.06	0.1900	ATP synthase, F0 complex, subunit G
Cox4i1	SPU_014478	−1.68 → −1.17	0.0597	Cytochrome C oxidase
Ndufb7	SPU_003071	−1.59 → −1.11	0.1133	NADH dehydrogenase
Ndufs1	SPU_013644	−1.60 → −1.12	0.1044	NADH dehydrogenase Fe-S protein 1
Ndufa12	SPU_002128	−1.52 → −1.09	0.1864	NADH dehydrogenase
Slc25a4	SPU_014660	−1.78 → −1.24	**0.0274**	ADP,ATP carrier protein 1
Biomineralization				
SM30-like	SPU_027906	−2.01 → −1.41	**0.0036**	Spicule matrix protein
SM29	SPU_005990	−1.60 → −1.12	0.1082	Spicule matrix protein
COLP3α	SPU_003768	−1.60 → −1.11	0.1090	Non-fibrillar collagen
Collagens	SPU_009076	−1.63 → −1.14	0.0853	Mostly fibrillar collagens
Cyclophilins	SPU_008305	−1.57 → −1.10	0.1293	Peptidylpropyl *cis-trans* isomerase
Osteonectin	SPU_028275	−1.97 → −1.38	**0.0050**	Mammalian SPARC-related genes
P19	SPU_004136	−1.56 → −1.09	0.1392	PMC-specific protein
Projectin	SPU_013917	−1.62 → −1.13	0.0928	Cytoskeletal kinase
Cellular stress & defensome				
Ubiquitin	SPU_015276	−1.60 → −1.12	0.1043	Ub-Proteasome
HIP1	SPU_010488	−1.72 → −1.20	**0.0439**	Chaperone cofactor, regulates JNK pathway
GST sigma	SPU_025323	−1.61 → −1.12	0.1016	Glutathione-S-Transferase, cytosolic
Gpx1	SPU_004397	−1.57 → −1.10	0.1256	Glutathione peroxidase 7
Gpx2	SPU_014276	−1.53 → −1.07	0.1689	Glutathione peroxidase 4
Fmo5	SPU_028586	−1.97 → −1.37	**0.0056**	Flavoprotein monooxygenase
Keap1	SPU_011306	−2.08 → −1.45	**0.0021**	Oxidative stress transcription factors
Aldh1-like1	SPU_002650	−2.46 → −1.72	**0.0001**	Oxidoreductase involved in redox regulation
Fth	SPU_004876	−1.62 → −1.14	0.0856	Ferritin heavy chain, iron storage
Calcineurin b	SPU_017036	−1.55 → −1.08	**0.0044**	Activates transcription of IL-2
Hsp40F	SPU_021154	+1.52 → +1.06	0.1860	Co-chaperone of Hsp70
Fmo3	SPU_017374	+1.60 → +1.12	0.1021	Flavoprotein monooxygenase
Acid-base & ion regulation				
Slco3a1	SPU_005806	−2.33 → −1.62	**0.0002**	Organic anion transporter
Atp1a3	SPU_025815	−1.61 → −1.12	0.1008	Na^+/K^+ ATPase
Atp8a1	SPU_019141	−1.73 → −1.21	**0.0387**	Class I, type 8 ATPase
Atp2a1	SPU_006779	+1.81 → +1.26	**0.0210**	Ca^{2+} ATPase
Atp13a3	SPU_015142	+1.53 → +1.07	0.1657	H^+/K^+ ATPase
Atp7a	SPU_028504	+1.51 → +1.06	0.1898	Cu^{2+} ATPase
Slc4a3	SPU_018701	+1.51 → +1.05	0.1956	Bicarbonate transporter
Protein synthesis — translational control				
eEF3e	SPU_007226	−1.63 → −1.14	0.0827	Translation initiation factor
eEF1Bδ	SPU_000960	−1.79 → −1.25	**0.0255**	Translation elongation factor
eEF1Bγ	SPU_002587	−1.70 → −1.18	0.0520	Translation elongation factor

2009) that focused on a very limited set of genes, especially molecular chaperones. In order to shed some light on the broad and integrated mechanisms underlying the observed morphological effects in *L. pictus*, we used a DNA microarray to assess how the transcriptome changed in the larvae raised under elevated CO_2. This transcriptomics approach (see Todgham & Hofmann 2009) has allowed us to capture the changes in gene expression that characterize the initial response to elevated CO_2 and provides insight into whether these developing larvae have the capacity to compensate at the molecular level for the effects of elevated CO_2.

Overall we found a general down-regulation of gene expression in urchin larvae that developed under High CO_2 conditions with almost 80% of the transcripts showing the largest changes in gene expression being down-regulated (Table 4). This includes a number of genes that are involved in biomineralization and skeletogenesis in developing urchin larvae (for review see Killian & Wilt 2008). Specifically, mRNA transcripts that encode for spicule matrix proteins, SM30-like and SM29, which are involved in the formation of the organic matrix of the larval spicule (Livingston et al. 2006) were down-regulated in urchin larvae exposed to High CO_2. Similarly the gene expression of a number of proteins that play an important role in skeleton elongation and growth such as collagens (Benson et al. 1990), a cyclophilin (Amore & Davidson 2006), P19 (Illies et al. 2002), and the Ca^{2+} binding protein osteonectin (Livingston et al. 2006) were also down-regulated in larvae exposed to High CO_2. Taken together, the transcriptomic results demonstrate that these larvae are not increasing the expression of genes coding for proteins that are critical to skeletogenesis to compensate for the effects of CO_2 on the biomineralization process.

In addition, the expression profiles of a large number of the genes involved in energy supply (ATP-generating) and demand (ATP-utilizing) are also down-regulated, consistent with what would be expected from an animal that has undergone a depression in metabolism (for review, see Storey & Storey 2007). There was subtle but widespread down-regulation in expression of genes involved in generating ATP through oxidative metabolism (e.g. the succinyl-CoA *Suclg1* of the TCA cycle and the ATP synthase *Atp5b* of the electron transport chain). Furthermore, larvae raised under High CO_2 conditions down-regulated a number of genes involved in the translation of proteins, such as elongation factors (e.g. *eEF1Bδ*), as well as the expression of Na^+/K^+-ATPase (Table 4), 2 biochemical processes with the greatest metabolic demand on developing sea urchin larvae (Leong & Manahan 1997, Pace & Manahan 2006). The microarray results of this study suggest that these larvae could be decreasing their metabolic activity to better cope with the high CO_2 environment. The combined decrease in expression of a number of biomineralization genes as well as those genes involved in energy metabolism may be potential mechanisms underlying the reduced skeleton formation in larvae exposed to elevated CO_2. Combined with similar work on closely related urchin species (*Strongylocentrotus purpuratus;* Todgham & Hofmann 2009), these results provide further evidence that larval sea urchins may not be able to buffer the effects of elevated CO_2 by up-regulating pathways important in skeletal growth.

While the majority of the largest transcriptomic changes were measured as decreased gene expression in larvae exposed to elevated CO_2, there were a small number of transcripts that were up-regulated in these larvae in response to increased levels of CO_2. Within this group of transcripts were 2 genes, an H^+/K^+-ATPase (*Atp13a3*) and a bicarbonate transporter (*Slc4a3*), that are involved in acid-base regulation. At present, there is very little information about the capacity of early developmental stages to cope with the acid-base disturbances associated with elevated CO_2. Research conducted on adult urchins (e.g. Spicer 1995, Burnett et al. 2002, Miles et al. 2007) suggests that these species, like most other invertebrates, are poor acid-base compensators. The microarray results of this study suggest that there may be an acid-base disturbance associated with exposure to CO_2 conditions that approximates future OA conditions and that these larval urchins are responding by up-regulating ion transporters involved in acid-base balance.

Although OA is often thought of as a process with very long time scales, recent work illustrates the importance of OA within the development time of individuals. Feely et al. (2008) documented upwelling-caused shoaling of corrosive water into shallow waters along the west coast of North America. In fact, Feely et al.'s (2008) study demonstrated that even the pH levels from the High CO_2 treatment in this experiment are within the range that organisms currently experience during upwelling conditions. On the one hand, this could suggest that our experimental conditions are simply part of the natural environment for echinoid larvae. On the other hand, if, as some investigators have suggested, surface ocean pH levels are trending lower in this environment (Wootton et al. 2008), then the shifts in larval size and gene expression patterns may also be part of a new reality.

The high-temporal variability of ocean pH highlights the need to understand how the developmental processes altered here might respond to changes in pH and carbonate saturation through time. It may be that, once the low pH, low carbonate water is removed

(such as with the relaxation of upwelling), larvae would be able to 'catch up' as they progress through their developmental program. However, it is likely that the deleterious impacts on the endoskeleton are irreversible and developmental canalization results in a permanently altered phenotype of a shorter, smaller body. The arm length in echinopluteus larvae is a well-known example of phenotypic plasticity in ecological development, and the reversal of these developmental trajectories is generally not possible (Boidron-Metairon 1988, Sewell et al. 2004, Sultan 2007).

Biological systems will respond to acidified oceans at several levels, including physiological and biochemical shifts, gross morphological changes in individuals, and ecological shifts in species distributions. To date, much of the attention has focused on biomineralization processes. The results presented here confirm the susceptibility of skeleton formation to slight changes in environmental pH. The ΔpHs in this experiment are lower than those used in similar studies (e.g. Dupont et al. 2008, Kurihara 2008); although the Control CO_2 treatment had a lower pH than expected for surface waters in equilibrium with air, the span between treatments was modest compared with comparable studies. As has been observed in another urchin species, the gene expression data provide evidence that echinoderms may not be able to compensate for elevated CO_2 levels through up-regulation of biomineralization genes. The broader evidence of metabolic depression indicates that OA could have more severe impacts on echinoderm larvae than a singular focus on skeletal growth would reveal. By providing us with a snapshot of the larval transcriptome during a period of skeletal growth, these results provide direction for future work to understand more broadly the physiological costs associated with developing under CO_2-acidified conditions and what cellular pathways are responding to modest increases in CO_2.

In summary, looking at the combination of gene expression levels concurrently with morphometric data demonstrates that the gross morphological changes seen in many organisms grown under acidified conditions are not the sole consequences of altered carbonate chemistry. This is not surprising; CO_2 and pH are critical components of organismal physiology (e.g. Pörtner 2008). These results suggest that morphological changes are symptomatic of broader challenges to the physiological state of echinoderm larvae and highlight the utility of integrated experiments combining assessment of multiple organismal characteristics.

Acknowledgements. We thank the Hofmann lab, especially T. Crombie, for assistance in collecting samples. E. Carpizo-Ituarte helped with the design of the larval culture chambers. We are grateful to Dr. Andrew Dickson's lab group for water sample analysis. Salinity and SST data were provided through the Santa Barbara Channel-Long Term Ecological Research and the Southern California Coastal Ocean Observing System (SCCOOS). Research was supported by NSF grant OCE-0425107 to G.E.H., an NSF International Postdoctoral Research Fellowship to N.A.F., an NSF Graduate Research Fellowship to L.M.H., and a University of California Marine Council, Coastal Environmental Quality Initiative Graduate Student Fellowship to M.L.Z. This is contribution number 334 from PISCO, the Partnership for Interdisciplinary Studies of Coastal Oceans funded primarily by the Gordon and Betty Moore Foundation and David and Lucile Packard Foundation.

LITERATURE CITED

Allen JD (2008) Size-specific predation on marine invertebrate larvae. Biol Bull 214:42–49

Amore G, Davidson EH (2006) *cis*-Regulatory control of cyclophilin, a member of the ETS-DRI skeletogenic gene battery in the sea urchin embryo. Dev Biol 293:555–564

Anderson MJ, Gorley RN, Clarke KR (2008) PERMANOVA+ for PRIMER: guide to software and statistical methods. PRIMER-E, Plymouth

Anthony KRN, Kline DI, Diaz-Pulido G, Dove S, Hoegh-Guldberg O (2008) Ocean acidification causes bleaching and productivity loss in coral reef builders. Proc Natl Acad Sci USA 105:17442–17446

Benson S, Smith L, Wilt F, Shaw R (1990) The synthesis and secretion of collagen by cultured sea urchin micromeres. Exp Cell Res 188:141–146

Bibby R, Cleall-Harding P, Rundle S, Widdicombe S, Spicer J (2007) Ocean acidification disrupts induced defences in the intertidal gastropod *Littorina littorea*. Biol Lett 3: 699–701

Boidron-Metairon IF (1988) Morphological plasticity in laboratory-reared echinoplutei of *Dendraster excentricus* (Eschscholtz) and *Lytechinus variegatus* (Lamarck) in response to food conditions. J Exp Mar Biol Ecol 119: 31–41

Burnett L, Terwilliger N, Carroll A, Jorgensen D, Scholnick D (2002) Respiratory and acid-base physiology of the purple sea urchin, *Strongylocentrotus purpuratus*, during air exposure: presence and function of a facultative lung. Biol Bull 203:42–50

Caldeira K, Wickett ME (2005) Ocean model predictions of chemistry changes from carbon dioxide emissions to the atmosphere and ocean. J Geophys Res 110:C09S04

Chomczynski P, Sacchi N (1987) Single-step method of RNA isolation by acid guanidinium thiocyanate-phenol-chloroform extraction. Anal Biochem 162:156–159

Clark D, Lamare M, Barker M (2009) Response of sea urchin pluteus larvae (Echinodermata: Echinoidea) to reduced seawater pH: a comparison among a tropical, temperate, and a polar species. Mar Biol 156:1125–1137

Cooper TF, De'Ath G, Fabricius KE, Lough JM (2008) Declining coral calcification in massive *Porites* in two nearshore regions of the northern Great Barrier Reef. Glob Change Biol 14:529–538

Cossins AR, Crawford DL (2005) Fish as models for environmental genomics. Nat Rev Genet 6:324–333

Dickson AG, Sabine CL, Christian JR (eds) (2007) Guide to best practices for ocean CO_2 measurements. PICES Spec Publ 3. Oak Ridge National Laboratory, Oak Ridge, TN, http://cdiac.ornl.gov/oceans/Handbook_2007.html

Doney SC, Fabry VJ, Feely RA, Kleypas JA (2009) Ocean acidification: the other CO_2 problem. Ann Rev Mar Sci 1:169–192

Dupont S, Havenhand J, Thorndyke W, Peck L, Thorndyke M (2008) Near-future level of CO_2-driven ocean acidification radically affects larval survival and development in the brittlestar *Ophiothrix fragilis.* Mar Ecol Prog Ser 373:285–294

Fabry VJ (2008) Marine calcifiers in a high-CO_2 ocean. Science 320:1020–1022

Fabry VJ, Seibel BA, Feely RA, Orr JC (2008) Impacts of ocean acidification on marine fauna and ecosystem processes. ICES J Mar Sci 65:414–432

Feely RA, Sabine CL, Hernandez-Ayon JM, Ianson D, Hales B (2008) Evidence for upwelling of corrosive 'acidified' water onto the continental shelf. Science 320:1490–1492

Goldstone JV, Hamdoun A, Cole BJ, Howard-Ashby M and others (2006) The chemical defensome: environmental sensing and response genes in the *Strongylocentrotus purpuratus* genome. Dev Biol 300:366–384

Gracey AY (2007) Interpreting physiological responses to environmental change through gene expression profiling. J Exp Biol 210:1584–1592

Guinotte JM, Orr J, Cairns S, Freiwald A, Morgan L, George R (2006) Will human-induced changes in seawater chemistry alter the distribution of deep-sea scleractinian corals? Front Ecol Environ 4:141–146

Hall-Spencer JM, Rodolfo-Metalpa R, Martin S, Ransome E and others (2008) Volcanic carbon dioxide vents show ecosystem effects of ocean acidification. Nature 454:96–99

Halpern BS, Walbridge S, Selkoe KA, Kappel CV and others (2008) A global map of human impact on marine ecosystems. Science 319:948–952

Hart MW, Strathmann RR (1994) Functional consequences of phenotypic plasticity in echinoid larvae. Biol Bull 186: 291–299

Hauton C, Tyrrell T, Williams JE (2009) The subtle effects of sea water acidification on the amphipod *Gammarus locusta.* Biogeosciences Discuss 6:919–946

Havenhand JN, Buttler FR, Thorndyke MC, Williams JE (2008) Near-future levels of ocean acidification reduce fertilization success in a sea urchin. Curr Biol 18:R651–R652

Hoegh-Guldberg O, Mumby PJ, Hooten AJ, Steneck RS and others (2007) Coral reefs under rapid climate change and ocean acidification. Science 318:1737–1742

Hughes TP, Reed DC, Boyle MJ (1987) Herbivory on coral reefs: community structure following mass mortalities of sea urchins. J Exp Mar Biol Ecol 113:39–59

Illies MR, Peeler MT, Dechtiaruk AM, Ettensohn CA (2002) Identification and developmental expression of new biomineralization proteins in the sea urchin *Strongylocentrotus purpuratus*. Dev Genes Evol 212:419–431

IPCC (2001) Climate change 2001: synthesis report. A contribution of Working Groups I, II, and III to the Third Assessment Report of the Intergovernmental Panel on Climate Change, Cambridge University Press, Cambridge

Killian CE, Wilt FH (2008) Molecular aspects of biomineralization of the echinoderm endoskeleton. Chem Rev 108: 4463–4474

Kuffner IB, Andersson AJ, Jokiel PL, Rodgers Ku S, Mackenzie FT (2008) Decreased abundance of crustose coralline algae due to ocean acidification. Nat Geosci 1:114–117

Kurihara H (2008) Effects of CO_2-driven ocean acidification on the early developmental stages of invertebrates. Mar Ecol Prog Ser 373:275–284

Kurihara H, Shirayama Y (2004) Effects of increased atmospheric CO_2 on sea urchin early development. Mar Ecol Prog Ser 274:161–169

Kurihara H, Shimode S, Shirayama Y (2004) Sub-lethal effects of elevated concentration of CO_2 on planktonic copepods and sea urchins. J Oceanogr 60:743–750

Langdon C, Atkinson MJ (2005) Effect of elevated pCO_2 on photosynthesis and calcification of corals and interactions with seasonal change in temperature/irradiance and nutrient enrichment. J Geophys Res 110:C09S07, doi: 10.1029/2004JC002576

Lee K, Tong LT, Millero FJ, Sabine CL and others (2006) Global relationships of total alkalinity with salinity and temperature in surface waters of the world's oceans. Geophys Res Lett 33:L19605, doi:10.1029/2006GL027207

Leong P, Manahan D (1997) Metabolic importance of Na^+/K^+-ATPase activity during sea urchin development. J Exp Biol 200:2881–2892

Livingston BT, Killian CE, Wilt F, Cameron A and others (2006) A genome-wide analysis of biomineralization-related proteins in the sea urchin *Strongylocentrotus purpuratus.* Dev Biol 300:335–348

McNeil BI, Matear RJ (2006) Projected climate change impact on oceanic acidification. Carbon Balance Manag 1:2, doi:10.1186/1750-0680-1-2

Mehrbach C, Culberson CH, Hawley JE, Pytkowicz RM (1973) Measurement of the apparent dissociation constants of carbonic acid in seawater at atmospheric pressure. Limnol Oceanogr 18:897–907

Miles H, Widdicombe S, Spicer JI, Hall-Spencer J (2007) Effects of anthropogenic seawater acidification on acid-base balance in the sea urchin *Psammechinus miliaris.* Mar Pollut Bull 54:89–96

O'Donnell MJ, Hammond L, Hofmann GE (2009) Predicted impact of ocean acidification on a marine invertebrate: elevated CO_2 alters response to thermal stress in sea urchin larvae. Mar Biol 156:439–446

Orr JC, Fabry VJ, Aumont O, Bopp L and others (2005) Anthropogenic ocean acidification over the twenty-first century and its impact on calcifying organisms. Nature 437:681–686

Pace DA, Manahan DT (2006) Fixed metabolic costs for highly variable rates of protein synthesis in sea urchin embryos and larvae. J Exp Biol 209:158–170

Pearse JS (2006) Ecological role of purple sea urchins. Science 314:940–941

Pennington JT, Strathmann RR (1990) Consequences of the calcite skeletons of planktonic echinoderm larvae for orientation, swimming, and shape. Biol Bull 179:121–133

Pierrot D, Lewis E, Wallace DWR (2006) MS Excel program developed for CO_2 system calculations. Carbon Dioxide Information Analysis Center, Oak Ridge National Laboratory, Oak Ridge, TN

Place SP, O'Donnell MJ, Hofmann GE (2008) Gene expression in the intertidal mussel *Mytilus californianus*: physiological response to environmental factors on a biogeographic scale. Mar Ecol Prog Ser 356:1–14

Pörtner HO (2008) Ecosystem effects of ocean acidification in times of ocean warming: a physiologist's view. Mar Ecol Prog Ser 373:203–217

Quinn P, Bowers RM, Zhang X, Wahlund TM, Fanelli MA, Olszova D, Read BA (2006) cDNA microarrays as a tool for identification of biomineralization proteins in the coccolithophorid *Emiliania huxleyi* (Haptophyta). Appl Environ Microbiol 72:5512–5526

R Development Core Team (2008) A language and environment for statistical computing. R Foundation for Statistical Computing, Vienna

Sea Urchin Genome Sequencing Consortium (2006) The genome of the sea urchin *Strongylocentrotus purpuratus.* Science 314:941–952

Sewell MA, Cameron MJ, McArdle BH (2004) Developmental plasticity in larval development in the echinometrid sea

urchin *Evechinus chloroticus* with varying food ration. J Exp Mar Biol Ecol 309:219–237

Shirayama Y, Thornton H (2005) Effect of increased atmospheric CO_2 on shallow water marine benthos. J Geophys Res 110:C09S08

Siegel DA, Mitarai S, Costello CJ, Gaines SD, Kendall BE, Warner RR, Winters KB (2008) The stochastic nature of larval connectivity among nearshore marine populations. Proc Natl Acad Sci USA 105:8974–8979

Skirrow G, Whitfield M (1975) The effect of increases in the atmospheric carbon dioxide content on the carbonate ion concentration of surface ocean water at 25°C. Limnol Oceanogr 20:103–108

Smyth GK (2004) Linear models and empirical Bayes methods for assessing differential expression in microarray experiments. Stat Appl Genet Mol Biol 3:3, doi:10.2202/1544-6115.1027

Smyth GK (2005) Limma: linear models for microarray data. In: Gentleman R, Carey V, Huber W, Irizarry R, Dudoit S (eds) Bioinformatics and computational biology solutions using R and Bioconductor. Springer, New York, p 397–420

Spicer JI (1995) Oxygen and acid-base status of the sea urchin *Psammechinus miliaris* during environmental hypoxia. Mar Biol 124:71–76

Storey KB, Storey JM (2007) Tribute to P. L. Lutz: putting life on 'pause'—molecular regulation of hypometabolism. J Exp Biol 210:1700–1714

Strathmann RR (1971) The feeding behavior of planktotrophic echinoderm larvae: mechanisms, regulation, and rates of suspension feeding. J Exp Mar Biol Ecol 6:109–160

Strathmann MF (ed) (1987) Reproduction and development of marine invertebrates of the northern Pacific Coast: data and methods for the study of eggs, embryos, and larvae. University of Washington Press, Seattle, WA

Strathmann RR, Grünbaum D (2006) Good eaters, poor swimmers: compromises in larval form. Integr Comp Biol 46: 312–322

Sultan SE (2007) Development in context: the timely emergence of eco-devo. Trends Ecol Evol 22:575–582

Tegner MJ, Dayton PK (1981) Population structure, recruitment and mortality of two sea urchins (*Strongylocentrotus franciscanus* and *S. purpuratus*) in a kelp forest. Mar Ecol Prog Ser 5:255–268

Todgham AE, Hofmann GE (2009) Transcriptomic response of sea urchin larvae *Strongylocentrotus purpuratus* to CO_2-driven seawater acidification. J Exp Biol 212: 2579–2594

Watanabe JM, Harrold C (1991) Destructive grazing by sea urchins *Strongylocentrotus* spp. in a central California kelp forest: potential roles of recruitment, depth, and predation. Mar Ecol Prog Ser 71:125–141

Wilt FH (2002) Biomineralization of the spicules of sea urchin embryos. Zool Sci 19:253–261

Wootton JT, Pfister CA, Forester JD (2008) Dynamic patterns and ecological impacts of declining ocean pH in a high-resolution multi-year dataset. Proc Natl Acad Sci USA 105:18848–18853

Yang YH, Dudoit S, Luu P, Lin DM, Peng V, Ngai J, Speed TP (2002) Normalization for cDNA microarray data: a robust composite method addressing single and multiple slide systematic variation. Nucleic Acids Res 30:e15, doi: 10.1093/nar/30.4.e15

Editorial responsibility: Peter Edmunds, Northridge, California, USA

Submitted: February 26, 2009; Accepted: September 29, 2009
Proofs received from author(s): December 12, 2009